

INVESTIGATING THE SYMMETRY OF THE Q, T -CATALAN
POLYNOMIALS USING NEW STATISTICS ON PLANE BINARY
TREES, TRIANGULATIONS OF CONVEX POLYGONS, AND
PAIRED LATTICE PATHS

By

KRISTY LAUREN BEAM

A Thesis Submitted to the Graduate Faculty of

WAKE FOREST UNIVERSITY

in Partial Fulfillment of the Requirements

for the Degree of

MASTER OF ARTS

in the Department of Mathematics

May 2009

Winston-Salem, North Carolina

Approved By:

Fredric T. Howard, Ph.D., Advisor

Examining Committee:

James Kuzmanovich, Ph.D., Chairperson

Edward Allen, Ph.D.

Table of Contents

List of Figures	ii
Acknowledgments	iii
Abstract	iv
Chapter 1 Introduction	1
1.1 The Symmetric Group	1
1.2 The Ring of Symmetric Functions	2
1.2.1 Basics and Definitions	2
1.2.2 Bases for the Ring of Symmetric Functions	3
1.2.3 Changing from One Basis to Another	7
1.3 Representation Theory	9
1.3.1 The Symmetric Group	9
1.3.2 Basics and Definitions	9
1.3.3 Characters	12
1.3.4 Permutation Module Corresponding to λ	15
Chapter 2 Diagonal Harmonics	18
2.1 The Action of S_n on a Polynomial Ring	18
2.2 The Diagonal Harmonics and its Decomposition	18
Chapter 3 Combinatorial Representations	21
3.1 Dyck Paths	21
3.1.1 Statistics	21
3.1.2 The Sweep Map	25
3.1.3 Q, t -Catalan	28
3.2 Plane Binary Trees on $2n + 1$ Vertices	29
3.2.1 Weight Preserving Bijection	31
3.3 Triangulations of Convex $(n + 2)$ -gons	34
3.3.1 Weighted Bijection	36
3.4 Plattices of Length $(n + 1)$	37
3.4.1 Weighted Bijection	38
Bibliography	40
Vita	41

List of Figures

1.1	The Ferrers Diagram for $(5,4,4,2,1,1)$	4
1.2	A Young Tableau for $(5,4,4,2,1,1)$	4
1.3	A SSYT for $(5,4,4,2,1,1)$ with $\mu = (2, 1, 2, 4, 4, 1, 2, 1)$	5
1.4	The Conjugate of $\lambda = (5, 4, 4, 2, 1, 1)$	8
3.1	A Dyck Path of Length 14	21
3.2	A Dyck Path of Length 14 and area 18	22
3.3	A Dyck Path of Length 14 and Bounce 31	23
3.4	A Dyck Path of Length 14 and $dinv$ 37	24
3.5	A Bounce Path for $sw(\hat{D})$	26
3.6	$sw(\hat{D})$	28
3.7	A Dyck Path of Length 5 with $area = boun = dinv = 3$	28
3.8	The Five Dyck paths of Length 3	29
3.9	Three Trees on 7 Vertices	30
3.10	Plane Binary Tree with Tarea 6	31
3.11	A Dyck Path and Its Image Under f	32
3.12	A Depth First Search	33
3.13	The 5 Triangulations of a Pentagon	35
3.14	One Element Under the Bijection $h : P_{14} \rightarrow T_{14}$	35
3.15	The Parea of a 16-gon	36
3.16	Four Sets of Paired Lattice Paths	37
3.17	Plarea for Two Plattices of Length 8	38
3.18	The First Step of $j : D_n \rightarrow L_n$	38
3.19	$area(D) = plarea(j(D))$	39

Acknowledgments

I would like to thank the faculty and staff of the Math Department at Wake Forest University for their support, encouragement, insights, and motivation. I would especially like to thank my committee: Dr. Fred Howard, Dr. James Kuzmanovich, and Dr. Ed Allen for their willingness to challenge and assist me in my endeavor. Most importantly, I would like to thank my true advisor, Dr. Greg Warrington, who continued to work with me despite the fact that he moved to Vermont. I learned not only a lot about mathematics during the course of my research, but I also learned how to do research by reading more mathematical writings on my own than I ever had before. I could not have done this without the support of the Math Department, to include my office mates and other fellow graduate students.

The Math Department at Lenoir-Rhyne University succeeded in preparing me for my graduate studies. I am very grateful for the challenges Dr. Douglas Burkholder, Dr. Richard Hull, and Dr. Bjarne Berg set before me as they pushed me to do my best.

And most importantly, I would like to thank my family, especially Kevin Watkins, for always being supportive and allowing me to have these two years to pursue my Masters. I could not have done it without them.

Abstract

Kristy Lauren Beam

INVESTIGATING THE SYMMETRY OF THE q, t -CATALAN POLYNOMIALS
USING NEW STATISTICS ON PLANE BINARY TREES, TRIANGULATIONS
OF CONVEX POLYGONS, AND PAIRED LATTICE PATHS

Thesis under the direction of Gregory Warrington, Ph. D.

The Catalan numbers, C_n , count length n Dyck paths: paths in the xy -plane from $(0, 0)$ to (n, n) which never fall below the line $y = x$ and consist entirely of unit north and east steps. There are statistics $area$, $dinv$, and $boun$ on Dyck paths that allow us to construct the q, t -Catalan polynomials:

$$C_n(q, t) = \sum_{D \in D_n} q^{area(D)} t^{dinv(D)} = \sum_{D \in D_n} q^{area(D)} t^{boun(D)},$$

where the sum is over all length n Dyck paths. We know from Haglund, Haiman, and Garsia's work in representation theory that the q, t -Catalan polynomials are symmetric, however there is no combinatorial proof for why this is true. Fortunately, the Catalan numbers count over 160 other combinatorial objects which may provide a combinatorial explanation for the symmetry. We will study plane binary trees, triangulations of convex polygons, and particular paired lattice paths. Statistics which correspond to the statistics on Dyck paths will be introduced for these objects in hopes of providing a new approach to combinatorially explaining the symmetry of the q, t -Catalan polynomials.

Chapter 1: Introduction

1.1 The Symmetric Group

Definition 1. For a set $A = \{1, 2, \dots, n\}$ of n elements, a permutation σ is a bijection from A to itself. The set of all such permutations with composition as multiplication is the symmetric group, S_n .

We can express $\sigma \in S_n$ in three ways: *two-line notation*, *one-line notation*, and *cycle notation*:

Definition 2. The two-line notation of σ is the array

$$\sigma = \begin{array}{cccccc} 1 & 2 & 3 & \cdots & n \\ \sigma(1) & \sigma(2) & \sigma(3) & \cdots & \sigma(n) \end{array} .$$

Suppose $n = 5$ and $\hat{\sigma}$ is the permutation which is given by $\hat{\sigma}(1) = 3$, $\hat{\sigma}(2) = 2$, $\hat{\sigma}(3) = 5$, $\hat{\sigma}(4) = 1$, and $\hat{\sigma}(5) = 4$. The two-line notation for $\hat{\sigma}$ is then

$$\hat{\sigma} = \begin{array}{ccccc} 1 & 2 & 3 & 4 & 5 \\ 3 & 2 & 5 & 1 & 4 \end{array} .$$

Definition 3. The one-line notation of σ is the two-line notation with the top row ommitted.

The one-line notation for $\hat{\sigma}$ is then

$$\hat{\sigma} = 3 \ 2 \ 5 \ 1 \ 4 .$$

Definition 4. For any $i_0 \in A$, the sequence $i_0, \sigma(i_0), \sigma^2(i_0), \sigma^3(i_0), \dots$ eventually repeats. Let k_0 be the first positive power of σ such that $\sigma^{k_0}(i_0) = i_0$. This leads to $(i_0, \sigma(i_0), \sigma^2(i_0), \dots, \sigma^{k_0}(i_0))$, a cycle of length k_0 . Now take some $i_1 \in A$ that is not in the cycle of i_0 and create its cycle. If we continue this until all elements of A have been accounted for in some cycle, we get

$$\sigma = (i_0, \sigma(i_0), \sigma^2(i_0), \dots, \sigma^{k_0}(i_0))(i_1, \sigma(i_1), \sigma^2(i_1), \dots, \sigma^{k_1}(i_1)) \cdots (i_m, \sigma(i_m), \sigma^2(i_m), \dots, \sigma^{k_m}(i_m)) \quad (1.1)$$

which is the cycle notation for σ .

The cycle notations for $\hat{\sigma}$ is then

$$\hat{\sigma} = (1, 3, 5, 4)(2) = (1, 3, 5, 4).$$

If an element is fixed under a permutation, we can omit it from the cycle notation.

Definition 5. For $\sigma \in S_n$, the cycle type of σ is

$$(n^{c_n}, (n-1)^{c_{n-1}}, \dots, 2^{c_2}, 1^{c_1})$$

where c_i is the number of cycles of length i . If $c_i = 0$, we may omit i from our cycle type, and if c_j is a positive integer, we repeat j that many times in our cycle type.

For example, the cycle type for $\hat{\sigma}$ is

$$(5^0, 4^1, 3^0, 2^0, 1^1) = (4, 1),$$

while the cycle type for $\bar{\sigma} = (1, 3)(2, 4)(5) = (1, 3)(2, 4)$ is

$$(5^0, 4^0, 3^0, 2^2, 1^1) = (2, 2, 1).$$

Writing the cycle type in this way gives rise to a partition of n .

1.2 The Ring of Symmetric Functions

1.2.1 Basics and Definitions

Definition 6. A ring R is a set together with two binary operations addition $+$ and multiplication \times that satisfies the following conditions:

- (a) R is an abelian group under $+$,
- (b) \times is associative, and
- (c) for $a, b, c \in R$, $(a + b) \times c = (a \times c) + (b \times c)$ and $c \times (a + b) = (c \times a) + (c \times b)$.

The set of complex numbers, \mathbb{C} , forms a ring under the usual addition and multiplication. If we have a ring R , we can construct a polynomial ring $P_n = R[x]$ which is the set of all polynomials in x of degree less than or equal to n , with coefficients in R . To add polynomials, we add coefficients which have equal powers of x , and to multiply two polynomials f and g , we multiply each term in f by each term in g ,

and then add the results. This notion can be extended to polynomial rings of more than one variable, $R[x_1, x_2, \dots, x_n]$. We can then say that $P = \mathbb{C}[x_1, x_2, \dots, x_n]$ is a polynomial ring over \mathbb{C} .

Definition 7. For a group G and a set S , a group action of G on S is a map $G \times S \rightarrow S$ such that for all $s \in S$

(a) $e \circ s = s$ where e is the identity element of G , and

(b) $g \circ (h \circ s) = gh \circ s$ for all $g, h \in G$.

Definition 8. Let $f = f(x_1, x_2, \dots, x_n) \in P = \mathbb{C}[x_1, x_2, \dots, x_n]$. Let $\sigma \in S_n$ act on f by $\sigma \circ f = f(x_{\sigma(1)}, x_{\sigma(2)}, \dots, x_{\sigma(n)})$. It is easily checked that this is a group action of S_n on P . A symmetric function is any function $f \in P$ such that $\sigma \circ f = f$ for all $\sigma \in S_n$.

We can argue that the set of all symmetric functions together with the compositions of P is in fact a ring since it is a *subring* of P :

Definition 9. A subset of a ring R is a subring if it is closed under addition, subtraction, and multiplication.

1.2.2 Bases for the Ring of Symmetric Functions

In this section we will construct four bases (monomial functions, Schur functions, elementary symmetric functions, and complete homogeneous symmetric functions) for the ring of symmetric functions using objects known as *Semi-standard Young tableaux*. Most of this can be found in Fulton[1].

Semi-standard Young Tableaux

Definition 10. A partition λ of n , denoted $\lambda \vdash n$, is a vector of positive integers $\lambda = (\lambda_1, \lambda_2, \dots, \lambda_k)$ where $\lambda_i \geq \lambda_{i+1}$ for all $1 \leq i \leq k-1$ and $\sum_{i=1}^k \lambda_i = n$.

Definition 11. The Ferrers diagram for a partition $\lambda = (\lambda_1, \lambda_2, \dots, \lambda_k) \vdash n$ is a left-justified array of empty cells where λ_i is the number of cells in the i th row from the top of the diagram. This Ferrers diagram is said to have shape λ .

Therefore, there are n cells in the Ferrers diagram and each row is no longer than the row above it. For example, the partition $\lambda = (5, 4, 4, 2, 1, 1)$, which partitions 17, has as its Ferrers diagram Figure 1.1. Sometimes we may prefer to abbreviate λ as $(5, 4^2, 2, 1^2)$.

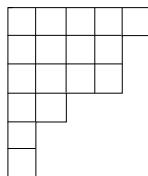


Figure 1.1: The Ferrers Diagram for $(5, 4, 4, 2, 1, 1)$

Definition 12. For $\lambda \vdash n$, a Young tableau of shape λ is a Ferrers diagram of shape λ where the cells have been filled in bijectively with the numbers $1, 2, \dots, n$.

There are $n!$ Young tableaux of shape λ . Figure 1.2 shows one Young tableau for $\lambda = (5, 4, 4, 2, 1, 1)$. Often we will omit the outline of the cells.

6	3	11	2	1
12	8	5	17	
14	7	9	10	
4	16			
15				
13				

Figure 1.2: A Young Tableau for $(5, 4, 4, 2, 1, 1)$

Definition 13. A generalized Young tableau of shape λ is a tableau which has been filled in with positive integers where repetitions are allowed. A generalized Young tableau T has content $\mu = (\mu_1, \mu_2, \dots, \mu_m)$ where μ_i is the number of times i appears in T .

A Young tableau has content $\mu = (1, 1, \dots, 1) = (1^n)$.

Definition 14. A generalized tableau is semi-standard if its columns strictly increase and its rows weakly increase. A standard tableau has both strictly increasing rows and columns, and therefore is a Young tableau.

Figure 1.3 is an example of a semi-standard Young tableau (SSYT) of shape $\lambda = (5, 4, 4, 2, 1, 1)$ with content $\mu = (2, 1, 2, 4, 4, 1, 2, 1)$.

1	1	3	4	4
2	3	4	5	
4	5	5	7	
5	6			
7				
8				

Figure 1.3: A SSYT for $(5,4,4,2,1,1)$ with $\mu = (2, 1, 2, 4, 4, 1, 2, 1)$

Monomial Symmetric Polynomials

Definition 15. Let $\lambda = (\lambda_1, \lambda_2, \dots, \lambda_k) \vdash n$. The monomial polynomial given by λ is

$$m_\lambda = \sum x_{i_1}^{\lambda_1} x_{i_2}^{\lambda_2} \dots x_{i_k}^{\lambda_k},$$

where the sum is over all distinct monomials having exponents $\lambda_1, \lambda_2, \dots, \lambda_k$.

For instance,

$$m_{(1,1)} = \begin{array}{l} x_1x_2 + x_1x_3 + x_1x_4 + \dots \\ x_2x_3 + x_2x_4 + x_2x_5 + \dots \\ x_3x_4 + x_3x_5 + x_3x_6 + \dots \\ \vdots \end{array} = \sum_{i < j} x_i x_j.$$

The monomial functions form an additive basis for the ring of symmetric functions.

Schur Functions

The *Schur polynomials* are symmetric polynomials which form an additive basis over the ring of symmetric polynomials. We will define them in terms of semi-standard Young tableaux. Given a semi-standard Young tableau T of shape λ filled with the integers 1 to m , define the monomial

$$x^T = \prod_{i=1}^m (x_i)^{\text{number of times } i \text{ occurs in } T}.$$

For T as in Figure 1.3 we have $x^T = x_1^2 x_2 x_3^2 x_4^4 x_5^4 x_6 x_7^2 x_8$. The content tells us the exponent for each variable. The Schur polynomial over m variables is then

$$s_\lambda(x_1, x_2, \dots, x_m) = \sum_T x^T$$

where the sum is over all semi-standard Young tableaux of shape λ filled with the numbers 1 to m . If we allow our semi-standard Young tableaux to be filled with any content, then we get the *Schur function*, s_λ , an additive basis of the ring of symmetric functions. It is not obvious that s_λ is a symmetric function, but for example, if $\lambda = (2, 1)$ and we limit ourselves to only using the numbers 1 through 3 to fill our semi-standard Young tableaux we obtain the following nine SSYT:

$$\begin{array}{ccc}
 \mathbf{1} & \mathbf{1} & \mathbf{1} & \mathbf{2} & \mathbf{1} & \mathbf{3} \\
 \mathbf{2} & & \mathbf{2} & & \mathbf{2} & \\
 \\
 \mathbf{1} & \mathbf{1} & \mathbf{1} & \mathbf{2} & \mathbf{1} & \mathbf{3} \\
 \mathbf{3} & & \mathbf{3} & & \mathbf{3} & \\
 \\
 \mathbf{2} & \mathbf{2} & \mathbf{2} & \mathbf{3} & & \\
 \mathbf{3} & & \mathbf{3} & & &
 \end{array} \quad (1.2)$$

Summing over x^T for each tableau, we get the Schur polynomial

$$s_{(2,1)} = x_1^2 x_2 + x_1 x_2^2 + 2x_1 x_2 x_3 + x_1^2 x_3 + x_1 x_3^2 + x_2^2 x_3 + x_2 x_3^2,$$

which is, in fact, $m_{(2,1)} + 2m_{(1,1,1)}$ with $x_i = 0$ for $i > 3$.

Elementary Symmetric Functions

If we let $\lambda = (1^n)$, then the Ferrers diagram associated with λ would be a single column with n rows. Any semi-standard Young tableau of shape (1^n) would have to consist of a sequence of strictly increasing positive integers down the single column. Thus, each positive integer can be used at most once in the filling of the tableau. Therefore, every exponent in x^T must be either a 0 or a 1 for any semi-standard Young tableau T of shape (1^n) . This gives us the Schur function

$$e_n = s_{(1^n)}$$

where e_n is the n th *elementary symmetric function*. The elementary symmetric function defined for $\lambda = (\lambda_1, \lambda_2, \dots, \lambda_k)$ is

$$e_\lambda = e_{\lambda_1} e_{\lambda_2} \cdots e_{\lambda_k}.$$

Complete Symmetric Functions

Similarly, for $\lambda = (n)$, we get the Ferrers diagram consisting of a single row of n boxes. Any semi-standard Young tableau of this shape would be comprised of a weakly increasing sequence of n positive integers. The only limit to how many times a certain element can be used to fill this diagram is the number of boxes remaining in the row. Thus, the only requirement on x^T is that it is a monomial with its exponents summing to n . Therefore the set $\{x^T : T \text{ is a semi-standard Young tableau of shape } (n)\}$ is the set of all distinct monomials of degree n . Thus the Schur function for $\lambda = (n)$ is

$$h_n = s_{(n)}$$

where h_n is the n th *complete symmetric function*. The complete symmetric function defined for λ is then

$$h_\lambda = h_{\lambda_1} h_{\lambda_2} \cdots h_{\lambda_k}.$$

1.2.3 Changing from One Basis to Another

Definition 16. *Let λ be a partition and μ be a sequence of nonnegative integers. Then $K_{\lambda\mu}$ is the number of semi-standard young tableaux of shape λ with content μ . If μ is a partition, we call $K_{\lambda\mu}$ a Kostka number.*

Definition 17. *Let F be the Ferrers diagram for $\lambda = (\lambda_1, \lambda_2, \dots, \lambda_k) \vdash n$. Then the conjugate of λ , denoted $\bar{\lambda}$, is the reflection of F about its main diagonal from upper left to lower right. That is $\bar{\lambda} = (\bar{\lambda}_1, \bar{\lambda}_2, \dots, \bar{\lambda}_{\lambda_1})$ where $\bar{\lambda}_i$ is the number of boxes in the i th column of F .*

One should note that if $\lambda \vdash n$, then $\bar{\lambda} \vdash n$ as well. For instance, counting the boxes in successive columns of the Ferrers diagram in Figure 1.1 for $\lambda = (5, 4, 4, 2, 1, 1)$ gives us $\bar{\lambda} = (6, 4, 3, 3, 1)$ whose Ferrers diagram is shown in Figure 1.4.

Using Kostka numbers and monomial polynomials can make calculating Schur polynomials easier. The following equation gives an alternate approach for determining the Schur polynomial for $\lambda \vdash n$.

$$s_\lambda = \sum_{\mu \vdash n} K_{\lambda\mu} m_\mu.$$

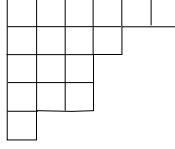


Figure 1.4: The Conjugate of $\lambda = (5, 4, 4, 2, 1, 1)$

Using this and the nine SSYT from (1.2) with partition content, we can expand s_λ in terms of monomials as

$$s_{(2,1)} = m_{(2,1)} + 2m_{(1,1,1)}. \tag{1.3}$$

There are similar equations for determining the other bases, $h_\mu(x)$ and $e_\mu(x)$, from the Schur functions. They are:

$$h_\mu = \sum_{\lambda} K_{\lambda\mu} s_\lambda, \text{ and}$$

$$e_\mu = \sum_{\lambda} K_{\bar{\lambda}\mu} s_\lambda.$$

These equations can simplify matters somewhat, but John Stembridge has a Maple package[7] for symmetric functions which allows for quicker conversions of bases. For instance, we can quickly determine that

$$h_{(4,3,2)} = s_{(9)} + 2s_{(8,1)} + 3s_{(7,2)} + s_{(7,1^2)} + 3s_{(6,3)} + 2s_{(6,2,1)} + 2s_{(5,4)} + 2s_{(5,3,1)} + s_{(5,2,2)} + s_{(4,4,1)} + s_{(4,3,2)}, \tag{1.4}$$

and

$$e_{(4,3,2)} = s_{(3^2,2,1)} + s_{(3^2,1^3)} + s_{(3,2^3)} + 2s_{(3,2^2,1^2)} + 2s_{(3,2,1^4)} + s_{(3,1^6)} + 2s_{(2^4,1)} + 3s_{(2^3,1^3)} + 3s_{(2^2,1^5)} + 2s_{(2,1^7)} + s_{(1^9)}. \tag{1.5}$$

If we were to calculate $h_{(4,3,2)}$ by hand we would need to determine $K_{\lambda(4,3,2)}$ for every $\lambda \vdash n$. For instance, in order to determine $K_{(6,3)(4,3,2)}$, we would need to draw all the semi-standard Young tableaux of shape $(6, 3)$ with content $(4, 3, 2)$. That is:

$$\begin{matrix} \mathbf{1} & \mathbf{1} & \mathbf{1} & \mathbf{1} & \mathbf{2} & \mathbf{2} & \mathbf{1} & \mathbf{1} & \mathbf{1} & \mathbf{1} & \mathbf{2} & \mathbf{3} & \mathbf{1} & \mathbf{1} & \mathbf{1} & \mathbf{1} & \mathbf{3} & \mathbf{3} \\ \mathbf{2} & \mathbf{3} & \mathbf{3} & & & & \mathbf{2} & \mathbf{2} & \mathbf{3} & & & & \mathbf{2} & \mathbf{2} & \mathbf{2} & & & \end{matrix},$$

in order to determine that $K_{(6,3)(4,3,2)}$, i.e. the coefficient of $s_{(6,3)}$ in the Schur polynomial expansion of $h_{(4,3,2)}$, is 3.

1.3 Representation Theory

1.3.1 The Symmetric Group

Definition 18. Let G be a group. For $g \in G$, the conjugacy class of g is $K_g = \{h \in G : khk^{-1} = g \text{ for some } k \in G\}$. We say that h and g are conjugates.

Conjugacy is an equivalence relation and therefore the conjugacy classes of a group G partition G . An important conjugacy class of the symmetric group S_n is the conjugacy class of transpositions.

Definition 19. A permutation $\tau = (i, j)$ of S_n where $i, j \in \{1, 2, \dots, n\}$ with $i \neq j$ is a transposition. The set of all such $\tau \in S_n$ is the conjugacy class of transpositions which generates all of S_n . For $\sigma = \tau_1, \tau_2, \dots, \tau_k \in S_n$, the sign of σ is $\text{sgn}(\sigma) = (-1)^k$.

The cycle type of a transposition is $\lambda = (2, 1^{n-2})$. In fact all of the conjugacy classes of S_n are comprised of permutations of the same cycle type and therefore we can index our conjugacy classes by cycle type. For example, the conjugacy class of transposition would be denoted $K_{(2, 1^{n-2})}$ and the conjugacy class of permutations of cycle type λ would be denoted K_λ .

1.3.2 Basics and Definitions

Definition 20. A matrix representation of a group G is a map $X : G \rightarrow \text{Mat}_d$, the set of $d \times d$ matrices, such that

(a) $X(e) = I_d$ where e is the identity element of G and I_d is the $d \times d$ identity matrix, and

(b) $X(gh) = X(g)X(h)$ for all $g, h \in G$.

That is, X is a homomorphism from G to the general linear group $GL_d = \{\text{all invertible } d \times d \text{ matrices}\}$. The degree, or dimension of X is d , denoted $\text{deg}X = d$.

For every group G there exists the *trivial representation*:

Definition 21. The trivial representation for a group G is the representation that sends every element of G to the matrix (1) . That is, $X(g) = (1)$ for all $g \in G$.

If we let our group be the symmetric group S_n , the map $sgn : S_n \rightarrow Mat_1$ is a one-dimensional representation. If $\sigma = (1, 4, 3, 2, 5) = (1, 5)(1, 2)(1, 3)(1, 4) \in S_5$, then $sgn(\sigma) = (-1)^4 = 1$. For S_n there also exists a degree n representation known as the *defining representation of S_n* :

Definition 22. Let $X : S_n \rightarrow GL_n$ by $X(\sigma) = (x_{i,j})_{n \times n}$ where

$$x_{i,j} = \begin{cases} 1, & \text{if } \sigma(j) = i; \\ 0, & \text{otherwise.} \end{cases}$$

Since each matrix is comprised of only 1's and 0's and there is a unique 1 in each row and column, then each of the matrices in the defining representation of S_n is a permutation matrix. The defining representation is illustrated below on one element of each cycle type of S_4 .

$$\begin{aligned} X(1, 2, 3, 4) &= \begin{pmatrix} 0 & 0 & 0 & 1 \\ 1 & 0 & 0 & 0 \\ 0 & 1 & 0 & 0 \\ 0 & 0 & 1 & 0 \end{pmatrix} & X(1, 4, 2) &= \begin{pmatrix} 0 & 1 & 0 & 0 \\ 0 & 0 & 0 & 1 \\ 0 & 0 & 1 & 0 \\ 1 & 0 & 0 & 0 \end{pmatrix} \\ X(2, 3)(1, 4) &= \begin{pmatrix} 0 & 0 & 0 & 1 \\ 0 & 0 & 1 & 0 \\ 0 & 1 & 0 & 0 \\ 1 & 0 & 0 & 0 \end{pmatrix} & X(2, 3) &= \begin{pmatrix} 1 & 0 & 0 & 0 \\ 0 & 0 & 1 & 0 \\ 0 & 1 & 0 & 0 \\ 0 & 0 & 0 & 1 \end{pmatrix} \\ X(e) &= \begin{pmatrix} 1 & 0 & 0 & 0 \\ 0 & 1 & 0 & 0 \\ 0 & 0 & 1 & 0 \\ 0 & 0 & 0 & 1 \end{pmatrix} \end{aligned}$$

Instead of thinking of representations in terms of matrices, we can think of them as *modules*:

Definition 23. Let V be a vector space and G be a group. V is a G -module if there exists a group homomorphism $\phi : G \rightarrow GL(V)$. We say that V carries a representation of G .

Definition 24. Let V be a G -module. A submodule of V is a subspace W that is closed under the action of G . That is, if $w \in W$ then $gw \in W$ for all $g \in G$. A non-trivial submodule of V is a submodule which is neither all of V nor $\{0\}$.

Definition 25. A non-zero G -module V is reducible if it contains a non-trivial submodule W . Otherwise, V is irreducible. Equivalently, V is reducible if it has a basis B in which every $g \in G$ yields a block matrix of the form

$$X(g) = \begin{pmatrix} A(g) & B(g) \\ 0 & C(g) \end{pmatrix},$$

where all the $A(g)$'s are the same size and 0 is a non-empty zero-matrix.

Definition 26. Let U and W be subspaces of V . Then V is the (internal) direct sum of U and W , $V = U \oplus W$, if every $\mathbf{v} \in V$ can be written uniquely as $\mathbf{v} = \mathbf{u} + \mathbf{w}$ for some $\mathbf{u} \in U$ and $\mathbf{w} \in W$. If V is a G -module and U and W are G -submodules then U and W complements.

The matrix analog of Definition 26 is that X is the *direct sum of matrices* A and B if

$$X = \begin{pmatrix} A & 0 \\ 0 & B \end{pmatrix}.$$

Theorem 1 (Maschke's Theorem). Let G be a finite group and let V be a finite-dimensional non-zero G -module. Then

$$V = W^{(1)} \oplus W^{(2)} \oplus \dots \oplus W^{(k)},$$

where each $W^{(i)}$ is an irreducible G -submodule of V .

The matrix representation analog of Mascke's Theorem is given in the following theorem.

Theorem 2. Let G be a finite group and X a matrix representation of G with degree $d > 0$. There exists a fixed matrix T such that for every $g \in G$ the matrix $X(g)$ has the form

$$TX(g)T^{-1} = \begin{pmatrix} X^{(1)}(g) & 0 & \dots & 0 \\ 0 & X^{(2)}(g) & \dots & 0 \\ \vdots & \vdots & \ddots & \vdots \\ 0 & 0 & \dots & X^{(k)}(g) \end{pmatrix}.$$

We say that a representation is *completely reducible* if it can be written as a direct sum of irreducibles.

Definition 27. Let V and W be G -modules. A G -homomorphism is a linear transformation $\theta : V \rightarrow W$ such that

$$\theta(g\mathbf{v}) = g\theta(\mathbf{v}).$$

A G -isomorphism is a G -homomorphism that is bijective, in which case we say V and W are G -equivalent.

1.3.3 Characters

Definition 28. Let $X(g)$ for $g \in G$ be a matrix representation. The character of X is

$$\chi(g) = \text{tr} X(g),$$

where tr is the trace of a matrix. If V is a G -module, the character of V is the character of a matrix representation X corresponding to V .

Since trace is invariant under conjugation it is a *class function*.

Proposition 1. Let X be a matrix representation of a group G of degree d with character χ . Then

- (a) $\chi(e) = d$ for e the identity element of G ;
- (b) If K is a conjugacy class of G , then for $g, h \in K$ we have $\chi(g) = \chi(h)$;
- (c) For a matrix representation Y of G with character ψ , if $X \cong Y$, then $\chi(g) = \psi(g)$ for all $g \in G$.

Since $\chi(g) = \chi(h)$ for all g and h in the same conjugacy class K of G , we can denote the character corresponding to K as $\chi_K = \chi(g)$ for any $g \in K$. We said earlier that conjugacy classes in S_n are determined by cycle type. Thus the characters of the defining representation of S_4 on each conjugacy class are:

$$\begin{aligned} \chi_{K_{(4)}} &= 0 & \chi_{K_{(3,1)}} &= 1 & \chi_{K_{(2,2)}} &= 0 \\ \chi_{K_{(2,1,1)}} &= 2 & \chi_{K_{(1,1,1,1)}} &= 4 & & \end{aligned}$$

Thus the character of the defining representation of S_n is the number of points left fixed by an element of the conjugacy class.

Definition 29. A character table is an array with row indexed by inequivalent irreducible characters of G and columns indexed by conjugacy classes. The (i, j) th entry of a character table is $\chi_{K_j}^{(i)}$ which is the i th character of the j th conjugacy class.

As of right now, we have three possible irreducible representations for S_4 . We can argue that the trivial representation and the sign representation are irreducible since they are one-dimensional and therefore can not be decomposed into representations of lesser degree. We will show later that the defining representation is not irreducible, but for the time being, assuming that is, we get a portion of the character table for S_4 as follows.

	$K_{(1,1,1,1)}$	$K_{(2,1,1)}$	$K_{(2,2)}$	$K_{(3,1)}$	$K_{(4)}$
χ^{triv}	1	1	1	1	1
χ^{sgn}	1	-1	1	1	-1
χ^{def}	4	2	0	1	0

The number of inequivalent irreducible representations of a group G is equal to the number of conjugacy classes of G , and therefore the character table for G is a square array. This is nice because once we know how many conjugacy classes there are for a group, we will know when to quit looking for more irreducible representations. Thus, there are five irreducible representations of S_4 .

Definition 30. Let χ and ψ be functions from a group G to the complex numbers \mathbb{C} . The inner product of χ and ψ is

$$\langle \chi, \psi \rangle = \frac{1}{|G|} \sum_{g \in G} \chi(g) \overline{\psi(g)},$$

where the bar over $\psi(g)$ means complex conjugation.

Proposition 2. Let χ and ψ be characters for a group G . Then

$$(a) \langle \chi, \psi \rangle = \frac{1}{|G|} \sum_{g \in G} \chi(g) \psi(g^{-1}),$$

(b) $\langle \chi, \psi \rangle = \frac{1}{|G|} \sum_K |K| \chi_K \overline{\psi_K}$, where the sum is taken over all conjugacy classes of G .

Since cycle type of permutations determines conjugacy classes in S_n , σ and σ^{-1} are in the same conjugacy class. Thus $\chi(\sigma) = \chi(\sigma^{-1})$ and

$$\langle \chi, \psi \rangle = \frac{1}{n!} \sum_{\sigma \in S_n} \chi(\sigma) \psi(\sigma) \tag{1.6}$$

for characters χ and ψ of S_n .

Definition 31. The Kronecker delta for a set S with an equivalence relation \cong is

$$\delta_{a,b} = \begin{cases} 1 & \text{if } a \cong b, \\ 0 & \text{otherwise,} \end{cases}$$

for $a, b \in S$.

Theorem 3 (Character Relations of the First Kind). *Let χ and ψ be irreducible representations of a group G , then*

$$\langle \chi, \psi \rangle = \delta_{\chi, \psi}.$$

Corollary 1. *Let X be a matrix representation of a group G with character χ . Suppose*

$$X \cong m_1 X^{(1)} \oplus m_2 X^{(2)} \oplus \cdots \oplus m_k X^{(k)}$$

where the $X^{(i)}$ are pairwise inequivalent irreducible representations of G with characters $\chi^{(i)}$ and $\deg X^{(i)} = d_i$.

(a) $\deg X = m_1 d_1 + m_2 d_2 + \cdots + m_k d_k$.

(b) $\chi = m_1 \chi^{(1)} + m_2 \chi^{(2)} + \cdots + m_k \chi^{(k)}$.

(c) $\langle \chi, \chi^{(j)} \rangle = m_j$ for all j .

(d) $\langle \chi, \chi \rangle = m_1^2 + m_2^2 + \cdots + m_k^2$.

(e) X is irreducible if and only if $\langle \chi, \chi \rangle = 1$.

(f) For Y a matrix representation of G with character ψ , $X \cong Y$ if and only if $\chi(g) = \psi(g)$ for all $g \in G$.

We can now show that the defining representation of S_4 is not irreducible. Using Equation 1.6 and Proposition 2 we get

$$\langle \chi^{def}, \chi^{def} \rangle = \frac{1}{4!} \sum_K |K| \chi_K \overline{\chi_K} = \frac{1}{24} (1 \cdot 4^2 + 6 \cdot 2^2 + 3 \cdot 0^2 + 8 \cdot 1^2 + 6 \cdot 0^2) = 2.$$

Thus, by part (e) of Corollary 1, the defining representation of S_4 is not irreducible.

Theorem 4 (Character Relations of the Second Kind). *Let K and L be conjugacy classes of group G . Then*

$$\sum_{\chi} \chi_K \overline{\chi_L} = \frac{|G|}{|K|} \delta_{K,L}$$

where the sum is taken over all irreducible characters of G .

The Character Relations of the Second Kind are inner products of columns of the character table for a group G , while the Character Relations of the First Kind are inner products of rows of the character table. The last few sections of Sagan's *The Symmetric Group*[5] provide enough theory to determine the character table for S_4 .

	$K_{(1,1,1,1)}$	$K_{(2,1,1)}$	$K_{(2,2)}$	$K_{(3,1)}$	$K_{(4)}$
χ^{triv}	1	1	1	1	1
χ^{sgn}	1	-1	1	1	-1
χ^3	2	0	2	-1	0
χ^4	3	1	-1	0	-1
χ^5	3	-1	-1	0	1

Using part (b) of Corollary 1 and a little bit of exploration, we see that

$$\chi^{def} = \chi^{triv} \oplus \chi^4.$$

1.3.4 Permutation Module Corresponding to λ

Chapter 2 of Sagan[5] describes how to find the irreducible representations of S_n for a general n by way of tabloid theory. We will not go into full detail here, but will briefly mention two special modules, the *permutation module* and the *Specht module*, which we will use in the next chapter.

Tabloids

Recall that a Young tableau of shape $\lambda \vdash n$ is a Ferrers diagram of λ that has been filled in bijectively with the numbers $1, 2, \dots, n$ with no limitations as with semi-standard Young tableaux.

Definition 32. A tabloid of shape λ , $\{t\}$, is a set of all Young tableaux of shape λ whose rows contain the same elements.

For example, for $\lambda = (3, 1)$ we have

$$\{t_1\} = \left\{ \begin{array}{cc|cc} 2 & 3 & 3 & 2 \\ 1 & & 1 & \end{array} \right\} = \overline{\frac{2 \ 3}{1}},$$

$$\{t_2\} = \left\{ \begin{array}{cc|cc} 1 & 3 & 3 & 1 \\ 2 & & 2 & \end{array} \right\} = \overline{\frac{1 \ 3}{2}},$$

$$\{t_3\} = \left\{ \begin{array}{cc} 1 & 2 \\ 3 & \end{array} , \begin{array}{cc} 2 & 1 \\ 3 & \end{array} \right\} = \frac{\overline{1 \ 2}}{\underline{3}}.$$

There is nothing special about the indexing of the $\{t_i\}$'s. We could have numbered them differently; I chose to let i correspond to the number in the second row for this example. Now $\sigma \in S_n$ acts on a Young tableau t of shape λ by permuting the entries of t . For example,

$$(1, 3, 2) \begin{array}{cc} 2 & 3 \\ 1 & \end{array} = \begin{array}{cc} 1 & 2 \\ 3 & \end{array}.$$

This induces an action of σ on tabloids by letting

$$\sigma\{t\} = \{\sigma t\}.$$

This gives rise to an S_n module.

Definition 33. *Let $\mu \vdash n$. Let*

$$M^\mu = S_n \{ \{t_1\}, \{t_2\}, \dots, \{t_k\} \},$$

where $\{t_1\}, \{t_2\}, \dots, \{t_k\}$ is a complete list of Young tableaux of shape μ . M^μ is the permutation module corresponding to λ .

These M^μ can be decomposed into irreducible *Specht modules* which are defined and discussed in Chapter 2 of Sagan. For $\lambda \vdash n$, the Specht modules, S^λ , form a complete list of irreducible S_n -modules over the complex field. A basis for S^λ is the set of *standard polytabloids*, which are a refinement on tabloids that correspond to tableaux with increasing rows and columns. An important theorem with combinatorial implications is Young's Rule.

Theorem 5 (Young's Rule). *The multiplicity of S^λ in M^μ is equal to the Kostka number from Section 1.2.3, that is*

$$M^\mu \cong \bigoplus_{\lambda} K_{\lambda\mu} S^\lambda. \tag{1.7}$$

For instance, if $\mu = (2, 2) \vdash 4$, then possible $\lambda \vdash 4$ are $(1, 1, 1, 1), (2, 1, 1), (2, 2), (3, 1), (4)$. $K_{(1,1,1,1)(2,2)} = K_{(2,1,1)(2,2)} = 0$ since there are no semistandard Young tableaux with

content $(2, 2)$ and greater than 2 rows. The multiplicity of the remaining λ are determined below.

$$\begin{array}{ccc}
 \lambda = (2, 2) & \lambda = (3, 1) & \lambda = (4) \\
 \mathbf{1} & \mathbf{1} & \\
 \mathbf{2} & \mathbf{2} & \\
 \mathbf{1} & \mathbf{1} & \mathbf{1} \\
 \mathbf{2} & & \mathbf{1} & \mathbf{1} & \mathbf{2} & \mathbf{2}
 \end{array} \tag{1.8}$$

Thus,

$$M^{(2,2)} = S^{(2,2)} \oplus S^{(3,1)} \oplus S^{(4)}.$$

Chapter 2: Diagonal Harmonics

James Haglund's book *The q, t -Catalan Numbers and the Space of Diagonal Harmonics*[2] is a great reference for the background material needed for this chapter and the next one.

2.1 The Action of S_n on a Polynomial Ring in $2n$ Variables

Let R_n denote a polynomial ring in $2n$ variables by defining $R_n = \mathbb{C}[x_1, \dots, x_n, y_1, \dots, y_n]$. R_n is an infinite dimensional vector space over \mathbb{C} with basis the set of all monomials. We define a group action of S_n on R_n by letting each $\sigma \in S_n$ act on each variable x_i by $\sigma \circ x_i = x_{\sigma(i)}$. And in turn, σ acts on each y_i in the same manner. This can be extended multiplicatively to all monomials and by linearity to all polynomials in R_n . Thus for $f \in R_n$, $\sigma \circ f(x_1, \dots, x_n, y_1, \dots, y_n) = f(x_{\sigma(1)}, \dots, x_{\sigma(n)}, y_{\sigma(1)}, \dots, y_{\sigma(n)})$. It should be clear that this action preserves the degree of each monomial since σ only permutes the indices and leaves the exponents alone. This action also preserves the *bi-degree* of each monomial:

Definition 34. For a monomial f in two sets of variables $\{x_i\}$ and $\{y_i\}$, the bi-degree of f is $\text{bideg}(f) = (h, k)$ where h is the degree in the x variables and k is the degree in the y variables.

Thus for any $f \in R_n$, $\sigma \circ f \in R_n$, so this action makes R_n into an S_n -module.

2.2 The Diagonal Harmonics and its Decomposition

Definition 35. We define the diagonal harmonics in R_n by

$$DH_n = \left\{ f \in R_n : \sum_{i=1}^n \frac{\partial^h}{\partial x_i^h} \frac{\partial^k}{\partial y_i^k} f = 0 \text{ for } 1 \leq h + k \leq n \right\}.$$

DH_n is a vector subspace of R_n . Given $f \in DH_n$ there exist some h and k such that $\sum \frac{\partial^h}{\partial x_i^h} \frac{\partial^k}{\partial y_i^k} f = 0$ and if we consider $\sigma \circ f$, we see that $\sum \frac{\partial^h}{\partial x_{\sigma(i)}^h} \frac{\partial^k}{\partial y_{\sigma(i)}^k} (\sigma \circ f) = 0$ so DH_n is an S_n -submodule of R_n . In fact, DH_n is a *doubly graded* S_n -submodule of R_n :

Definition 36. A doubly graded S_n -module V is a module with a direct sum decomposition

$$V = \bigoplus_{h \geq 0} \bigoplus_{k \geq 0} V_{h,k}$$

where each $V_{h,k}$ is an S_n -submodule of V .

The direct sum decomposition for DH_n is

$$DH_n = \bigoplus_{h \geq 0} \bigoplus_{k \geq 0} V_{h,k}(n)$$

where each $V_{h,k}(n) = \{f \in DH_n : \text{bideg}(f) = (h, k)\} \cup \{0\}$ is a submodule of DH_n . Since each $V_{h,k}(n)$ is finite dimensional, each one can be decomposed into direct sums of irreducible submodules. That is,

$$V_{h,k}(n) = \bigoplus_{\lambda \vdash n} c_{\lambda}^{h,k} S^{\lambda}$$

where $c_{\lambda}^{h,k}$ is a coefficient for how often each S^{λ} , the Specht module, appears in the decomposition. Each S^{λ} has its corresponding irreducible character χ^{λ} . Thus the character of each $V_{h,k}(n)$ is

$$\text{char}(V_{h,k}(n)) = \sum_{\lambda \vdash n} c_{\lambda}^{h,k} \chi^{\lambda}.$$

We can now take advantage of the *Frobenius map* which is an isomorphism from the set of representations of an S_n module to the ring of symmetric functions. We can define the Frobenius map on a basis for the set of representations and then extend by linearity for the remaining elements. Using the set of irreducible representations as our basis, the Frobenius map sends χ^{λ} to s_{λ} , where s_{λ} is a Schur function: a basis element for the ring of symmetric functions. The *Frobenius Characteristic* of each $V_{h,k}(n)$ is $\sum_{\lambda \vdash n} c_{\lambda}^{h,k} s_{\lambda}$. We now define the *Frobenius Series* of DH_n to be the weighted series

$$\mathcal{F}_{DH_n}(q, t) = \sum_{h,k \geq 0} \left(\sum_{\lambda \vdash n} c_{\lambda}^{h,k} s_{\lambda} \right) q^h t^k$$

which is contained in $\Lambda_{(q,t)}$. There is a linear operator *nabla*, ∇ , that allows us to compute the Frobenius Series of DH_n . The eigenfunctions for ∇ are the modified Macdonald Polynomials which are a basis for the ring of symmetric functions. The following is a major theorem in this field.

Theorem 6. $\nabla(e_n) = \mathcal{F}_{DH_n}(q, t)$.

More information on the derivation of this theorem can be found in Haglund[2]. Since $e_n = s_{1^n}$, we have that $\nabla(s_{1^n}) = \mathcal{F}_{DH_n}(q, t)$. The q, t -Catalan polynomials are symmetric polynomials of the form

$$C_n(q, t) = \sum_{h,k \geq 0} c_{1^n}^{h,k} q^h t^k.$$

Thus, the q, t -Catalan numbers tell us how many times the sign character occurs in each graded piece of the representation DH_n .

Chapter 3: Combinatorial Representations

3.1 Dyck Paths

Definition 37. A *Dyck Path* is a path in the (x, y) plane beginning at the point $(0, 0)$ and travelling to the point (n, n) by way of north and east steps such that the path never falls below the line $y = x$. Such a path is said to have length n .

In the above definition, a *north step* means a line segment of length one in the positive y -direction. Likewise, an *east step* is a line segment of length one in the positive x -direction. Thus a Dyck path of length n consists of n north steps and n east steps. Figure 3.1 is an example of a Dyck path of length 14.

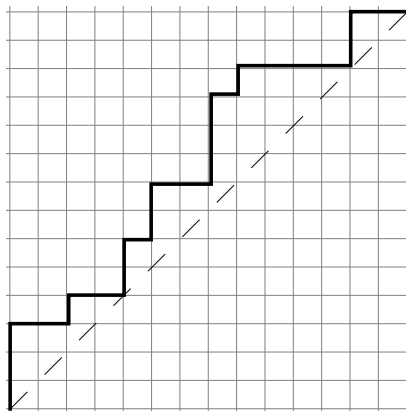


Figure 3.1: A Dyck Path of Length 14

3.1.1 Statistics

We can measure a Dyck path using different techniques. Each technique results in a specific measurement, or statistic. The first, and most natural, statistic which was first studied by MacMahon[4] is *area*. Area for a Dyck path is defined as the number of complete unit squares contained between the Dyck path and the line $y=x$. For instance, the Dyck path from Figure 3.2 has an area of 18. Note that we disregard any partial unit squares.

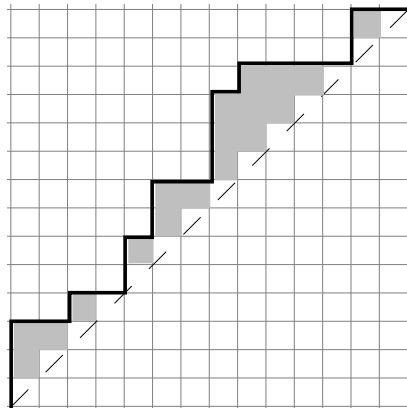


Figure 3.2: A Dyck Path of Length 14 and area 18

We can gain more information about a given Dyck path if we break down its total area into areas for each row of the Dyck path. For instance, the top row of our example Dyck path has area 1, while the second row from the top contributes no area to the overall area of the Dyck path. For convenience sake, we will label each row of our Dyck path from 1 to n with 1 being the bottom row, n being the top row, and i being the i th row from the bottom. We can construct what is known as the *g-vector* for a given Dyck path by defining $\vec{g} = (a_n, a_{n-1}, \dots, a_1)$ where a_i is the area which the i th row contributes to the total area. Thus the g-vector for our example is $g = (1, 0, 3, 3, 2, 1, 2, 1, 1, 0, 1, 2, 1, 0)$ and $\sum a_i = 18$. The g-vector for a Dyck path is a viable substitution for the pictorial representation of the Dyck path since each g-vector corresponds uniquely to its Dyck path. In general, a vector $\vec{v} = (v_n, v_{n-1}, \dots, v_1)$ of length n corresponds to a Dyck path of length n only if (1) each v_i is a nonnegative integer, (2) $v_i - v_{i-1} \leq 1$ for all $i \geq 1$, and (3) $v_i \leq i - 1$ for all i . Given a g-vector, the graph of the Dyck path can be constructed by first sketching in the portion of the line $y = x$ from $(0,0)$ to (n,n) as an aid and then placing the i th north step so that it starts at $(i - 1 - a_i, i - 1)$ and continues to $(i - 1 - a_i, i)$. The east steps should connect the top of a north step with the bottom of the next nonadjacent north step.

A second statistic on Dyck paths is *bounce*, sometimes abbreviated *boun*. Bounce was introduced by Haglund[3], and is a bit less intuitive than area, yet still has a nice visual representation. We can calculate bounce by first thinking of the path a billiard ball would take from (n, n) to $(0, 0)$ if the Dyck path and the line $y = x$ were the sides

of a pool table. The billiard ball initially travels to the west and continues to travel until it hits a vertical “wall,” at which point it takes an immediate turn to the south until it hits the line $y = x$. After hitting the diagonal line, the ball proceeds again to the west until hitting another vertical wall and this process continues until the ball arrives at the origin. We call the path of the billiard ball the *bounce path*. Now that we have our bounce path, we are ready to calculate the bounce. We are interested in the north steps with which the billiard ball makes perpendicular contact. In other words, we want to look at the north steps which cause the billiard ball to head south toward the diagonal. We can think of the amount each north step contributes to the total bounce, as the distance that north step prevents the ball from going, or more visually as the number of squares to the west of the the north step but still inside the $n \times n$ square.

Another, more useful way to count bounce is by keeping track of the length of each bounce in the west direction. If we start at the top of our Dyck path and label each row which contributes to the overall bounce with $j = 0, 1, 2 \dots$ and let b_j denote the length of the bounce, then in Figure 3.3, $b_0 = 2$, $b_1 = 4$, and so on. The vertical lines in Figure 3.3 are drawn in to illustrate that b_j contributes $j \cdot b_j$ to the total bounce. Therefore we can say that $b = \sum_j j \cdot b_j$. In our example Dyck path the total bounce is 31. In Figure 3.3, the bounce path is represented by the broken line and the bounce is shown by the gray boxes.

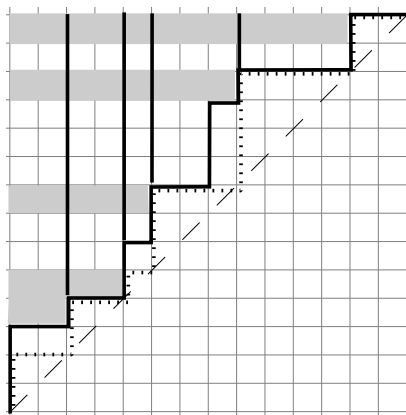


Figure 3.3: A Dyck Path of Length 14 and Bounce 31

The last statistic that we will talk about for the time being is *dinv*, which was introduced by Mark Haiman. The best way to visually understand *dinv* is as the total number of pairs of north steps where 1) both north steps lie on the same diagonal, or 2) the lower of the two north steps lies on the diagonal which is one step further from the line $y = x$ than the diagonal for the higher north step. As can be seen in the Figure 3.4, north steps 1, 2 and 3 all lie on the same diagonal, but $a, b, c, d, e,$ and f lie on the diagonal which is one step closer to the line $y = x$. Any unordered pair $\{1, 2\}, \{1, 3\},$ or $\{2, 3\}$ is counted for the *dinv* statistic. Since north step 1 is below $b, c, d, e,$ and f , 1 must be paired with each of these when compiling pairs for *dinv*. However, only the pairs $\{2, e\}, \{2, f\},$ and $\{3, f\}$ are valid for north steps 2 and 3.

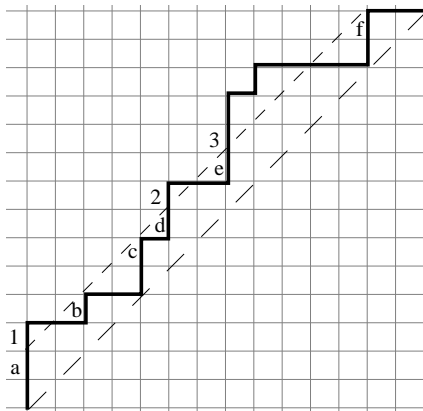


Figure 3.4: A Dyck Path of Length 14 and *dinv* 37

One could see how messy things could get trying to calculate *dinv* by drawing in multiple diagonals and pairing together north steps. In fact that is not how I determined that the *dinv* for our example is 37. Fortunately we can devise various approaches for calculating each statistic that might allow us a more natural and efficient way to think about and understand these statistics. On the other hand, we can also find approaches which complicate our calculations; typically we want to avoid these methods and search for a more desirable approach. Recall that the *g*-vector uniquely determines a Dyck path, so it must be the case that the *g*-vector contains adequate information for us to calculate *dinv*. Notice in Figure 3.4 above that north steps 1, 2, and 3 each contribute an area of 2 to the total area of the Dyck path. In fact all north steps on a given diagonal will contribute the same amount of

area to the total area. Conversely, if two north steps contribute the same amount of area, they must be on the same diagonal. Since north steps a, b, c, d, e , and f are on the diagonal one step closer to $y = x$, they each contribute an area of $2 - 1 = 1$ to the total area. If we now think of our g -vector as a column vector, as opposed to a row vector, we have the tools we need in order to calculate $dinv$ from the g -vector. For our example, $g = (1, 0, 3, 3, 2, 1, 2, 1, 1, 0, 1, 2, 1, 0)^t$ is the corresponding column vector. Since north steps with the same area are on the same diagonal, we must first count the number of ways we can pair together north steps of the same area. Letting $|a|$ be the number of a 's in our g -vector, this translates into $\binom{|a|}{2}$. To account for the pairs where the higher of the two north steps is on the diagonal one step closer to the line $y = x$, we must keep track of $|a \succ (a + 1)|$, the number of a 's above $a + 1$'s. Thus in general,

$$dinv = \sum_{i=0} \left[\binom{|i|}{2} + |i \succ i + 1| \right]. \quad (3.1)$$

Using Equation 3.1, for our example we calculate

$$dinv = \binom{3}{2} + 7 + \binom{6}{2} + 8 + \binom{3}{2} + 0 + \binom{2}{2} = 37.$$

We can also use the g -vector to calculate bounce, but I find this method to be less intuitive and more complicated than the method we used in Figure 3.3.

We have already seen to some extent how bounce and $dinv$ for Dyck paths are closely linked with area. In the next section, we will see even stronger evidence of the interconnectedness of these three statistics.

3.1.2 The Sweep Map

We can find a multitude of bijections from the set of length n Dyck paths, D_n , to itself. The bijections that are important to us are the ones that behave nicely with respect to the statistics area, $dinv$, and $boun$. In other words, we are not only concerned with where a bijection sends a Dyck path, D , but also what happens to $area(D)$, or one of the other statistics. For instance, a very nice bijection would be $\phi : D_n \rightarrow D_n$ such that $area(D) = dinv(\phi(D))$ and $dinv(D) = area(\phi(D))$ for all $D \in D_n$. Unfortunately no one has managed to define this bijection. However, there is a map known as the *Sweep Map* that has the following nice properties:

Proposition 3. *Let D_n be a Dyck path of length n and let sw denote the Sweep Map. Then $area(D_n) = boun(sw(D_n))$ and $dinv(D_n) = boun(sw(D_n))$.*

Proof. We define the Sweep Map in the following way to make these properties hold. Given a Dyck path D with g -vector $\vec{g} = (a_n, a_{n-1}, \dots, a_1)^t$, we first determine the number of i 's such that $a_i = 0$, then the number of i 's such that $a_i = 1$, and so on. We are now ready to draw in the bounce path for $sw(D)$. Starting at the point (n, n) , the billiard ball travels west one step for each 0 in the g -vector and then bounces south until it makes contact with the line $y = x$. Once this happens, the billiard ball again travels to the west, but this time going one step for each 1 in the g -vector and then it bounces back to the diagonal. The billiard ball continues in this manner until it reaches $(0, 0)$ and has accounted for all the values in the g -vector. Letting our Dyck path from Figure 3.1 be named \hat{D} , Figure 3.5 shows the bounce path for the sweep of \hat{D} .

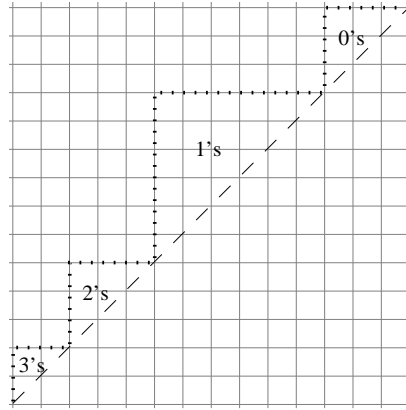


Figure 3.5: A Bounce Path for $sw(\hat{D})$

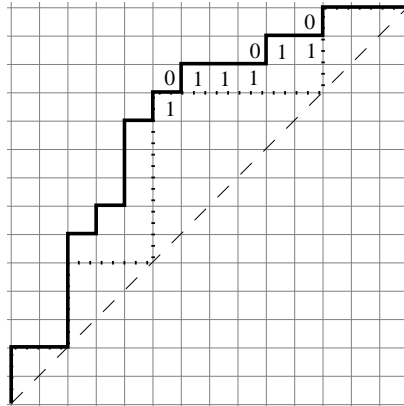
We can go ahead and see that the bounce for this new Dyck path will in fact be 18, which was the area of \hat{D} . Recalling that $boun = \sum_j j b_j$, we can see for the bounce path in Figure 3.5 that $boun = 0(3) + 1(6) + 2(3) + 3(2) = 18$ which is a direct consequence of there being three 0's, six 1's, three 2's, and two 3's in the g -vector for \hat{D} . It is also evident that the area enclosed by this bounce path comes directly from the portion of \hat{D} 's $dinv$ that corresponds to north steps on the same diagonal. For instance, the six 1's in \hat{D} 's g -vector contribute $\binom{6}{2}$ to the $dinv$. In $sw(\hat{D})$ they

account for an area of $5 + 4 + 3 + 2 + 1 + 0$. This is the fifth triangular number; the triangular numbers are given by $T_n = \binom{n+1}{2}$.

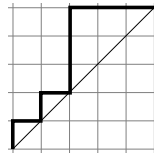
The remaining dinv is accounted for as we draw in the actual Dyck path for $sw(\hat{D})$. Starting at (n, n) , the first line of our Dyck path must include the entire top line of the bounce path and nothing more, in order for the bounce path to truly be a bounce path. After heading to the west by as many step as there are 0's in \vec{g} , we now must head south abiding by the following rules. Starting at the bottom of \vec{g} and working our way to the top, we take one step to the south as we arrive at each 0, one step to the west with each 1 we pass, and we do nothing for the other values in \vec{g} . This will take us to the corner of the bounce path dictated by the number of 1's in \vec{g} . Now we repeat the process, but now moving south for 1's and west for 2's. This process continues until we reach $(0, 0)$ and have worked our way through all the values of \vec{g} .

Condition (2) for determining if a length n vector is a g -vector guarantees that the first step in each of the sections is to the south (i.e. the first $a + 1$ in the g -vector is above at least one a) and thus agrees with the bounce path. Condition (2) says that $v_i - v_{i-1} \leq 1$ for all $i \geq 1$. Thus the entry below the first $a + 1$ must be an a , and therefore we certainly come to an a before we come to any $a + 1$ as we ascend through \vec{g} . In Figure 3.6 $sw(\hat{D})$ has been superimposed on its bounce path and the previous rules have been demonstrated for the 0,1-case. To facilitate clarity, vertical steps have been labeled with a 0 to the left and horizontal steps with a 1 underneath. Each north/south step corresponding to a is forced over one more step to the west (i.e. contributes one more unit of area) for each $a + 1$ that is below it in \vec{g} . Keeping in mind that being below an entry in \vec{g} results in being to the right of that entry in the picture of our Dyck path, the two 1's that are below the second 0 are also below the third 0, so they are each counted twice for the dinv of \hat{D} and twice for the area of $sw(\hat{D})$. \square

The Sweep Map helps to emphasize the dependency of bounce and dinv on area. One could argue that area is the only true statistic; dinv is merely the preimage of area under the Sweep Map and bounce the image. Any Dyck path that gets mapped to itself under the Sweep Map must have equal values for all three statistics. Figure 3.7 is an example of such a Dyck path. Having all three statistics the same is not enough

Figure 3.6: $sw(\hat{D})$

to guarantee the Dyck path is fixed by the Sweep Map. It is left to the reader to verify that Figure 3.7 is indeed fixed.

Figure 3.7: A Dyck Path of Length 5 with $area = boun = dinv = 3$

3.1.3 Q,t-Catalan

Many people are familiar with the *Catalan Numbers*, and know them as an infinite sequence which is defined by

$$C_n := \frac{1}{2n+1} \binom{2n+1}{n} = \frac{1}{n+1} \binom{2n}{n}, \quad (3.2)$$

where C_n denotes the n th Catalan Number. One of the objects which the n th Catalan number counts are length n Dyck paths. Using Equation 3.2, we can determine that $C_3 = 5$, and there are in fact five Dyck path of length 3. They are shown in Figure 3.8. Our running example has been a Dyck path of length 14; we had 2,674,440 choices of length 14 Dyck paths.

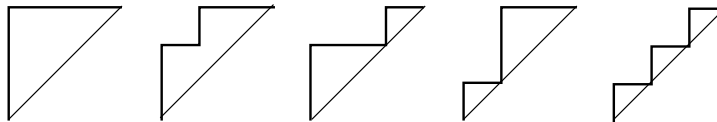


Figure 3.8: The Five Dyck paths of Length 3

The q,t -Catalan numbers are a refinement on the Catalan numbers, specifically they count weighted sums of Dyck paths. The q,t -Catalan numbers are actually polynomials which keep a record of how many Dyck paths have a certain area and a certain $dinv$ (or bounce). Mathematically speaking, let D_n denote the set of all length n Dyck paths, and then the q,t -Catalan polynomials can be expressed as

$$C_n(q, t) = \sum_{D \in D_n} q^{\text{area}(D)} t^{\text{dinv}(D)} \quad (3.3)$$

Thus the number of Dyck paths with $\text{area} = a$ and $\text{dinv} = d$ is the coefficient of $q^a t^d$ in $C_n(q, t)$. The total number of Dyck paths of length n would just be $C_n(1, 1)$, the sum of all the coefficients of $C_n(q, t)$. We know from work in Chapter 2 that $C_n(q, t)$ is in fact a symmetric polynomial, meaning $C_n(q, t) = C_n(t, q)$. Combinatorially this means that the number of Dyck paths with $\text{area} = a$ and $\text{dinv} = d$ is the same as the number of Dyck paths with $\text{area} = d$ and $\text{dinv} = a$. No one has yet to figure out a combinatorial reason why this must be so. However, Dyck paths are not the only objects that the Catalan numbers count. There are over 160 different objects which are counted by the Catalan numbers, many of which are described in Stanley's *Enumerative Combinatorics*[6]. The remainder of our time will be spent looking at three of these objects to see if we can find statistics on them which behave in the way area, bounce, and $dinv$ do for Dyck paths. This will give us possibly a new perspective from which to approach the symmetry issue.

3.2 Plane Binary Trees on $2n + 1$ Vertices

We will define a *plane binary tree* by showing how to construct one, but first we will need a few graph theory definitions which pertain to the theory of trees. The *degree* of a vertex, v , is the number of edges coming out of v . A critical aspect of a plane binary tree on $2n + 1$ vertices is that it has one vertex of degree 2, $n + 1$ vertices

of degree 1, and $n - 1$ vertices of degree 3. Let the *distance* between two vertices be the number of edges in the shortest route between the two vertices. We define the *level of a vertex*, denoted $lv(v)$, to be the distance from the vertex to the single vertex of degree two. We can then say that a *parent* of a vertex v is a vertex w with $lv(w) = lv(v) - 1$ that is connected to v by an edge. Likewise, a *child* of a vertex w is a vertex v with $lv(v) = lv(w) + 1$ that is connected to w . In a plane binary tree, all vertices are children except for the vertex of degree 2 and every parent vertex has exactly two children. The endpoints are the only non-parent vertices. We will say that a *family* is a parent vertex together with its two children.

We draw a plane binary tree by first drawing the single vertex, v_0 , of degree 2. Below this vertex we draw its two children vertices, which are the only two level 2 vertices, and the edges adjoining them to v_0 . We then add in all of the children of the level 2 vertices in the same manner and continue until we are out of vertices. This will give us a plane binary tree. However, this process does not yield a unique plane binary tree because we made no specifications on the order of vertices of the same level. For some trees, this is an unnecessary distinction, but plane binary trees are identical only if they look identical. For example, the two trees on the left in Figure 3.9 are distinct plane binary trees on 7 vertices, but the tree on the right is not a plane binary tree.

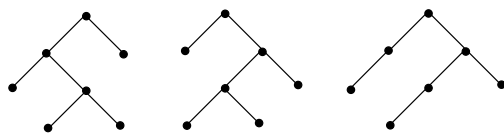


Figure 3.9: Three Trees on 7 Vertices

We can define a statistic on these plane binary trees that we will call *tarea*. Isolating the families of a plane binary tree will be useful in calculating *tarea* since *tarea* for the tree will be the sum of the *tarea* for each family. As a starting place, let the *tarea* of the family whose parent vertex has degree 2 be 0. Then descend down the tree in the following manner: if a family F comes off of the left child of a family of *tarea* = t then $tarea(F) = t + 1$; if F comes off of the right child of a family of *tarea* = t then $tarea(F) = t$. Summing over all the families of a plane binary tree yields the *tarea*

of the tree; that is for a tree T ,

$$\text{tarea}(T) = \sum_{F \in T} \text{tarea}(F).$$

An example of a plane binary tree with its corresponding tarea is shown in Figure 3.10. A plane binary tree on $2n + 1$ vertices is comprised of exactly n families. Let the set of all plane binary trees on $2n + 1$ vertices be denoted T_n . We will show in the next section, via a bijection, that the number of trees in T_n is C_n , the n th Catalan number.

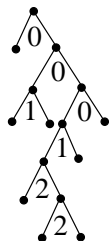


Figure 3.10: Plane Binary Tree with Tarea 6

3.2.1 Weight Preserving Bijection

Definition 38. Let A and B be sets of the same size with statistics α and β , respectively. A bijection $\phi : A \rightarrow B$ is a weight preserving bijection if $\alpha(a) = \beta(\phi(a))$ for all $a \in A$. Equivalently, if $\beta(b) = \alpha(\phi^{-1}(b))$ for all $b \in B$.

We will define a map from D_n to T_n , show that it is a bijection, and then show that it takes area to tarea . Let $f : D_n \rightarrow T_n$ be a map defined as follows. Let D be a Dyck path of length n . Since there are n north steps in D and n families in a plane binary tree on $2n + 1$ vertices, we force north steps to correspond to families. The n east steps of D correspond to n of the $n + 1$ endpoints of a plane binary tree. Starting at $(0, 0)$ on D and moving up the path to (n, n) we add a new family to our tree for each north step we enter and we declare that a specific vertex is an endpoint for each east step we enter. Starting at $(0, 0)$, our first step of D is always a north step, so we draw a family, f_1 . We now have a plane binary tree on 3 vertices. Any new family we add must be connected to what we have already drawn, and we can only declare vertices which we have already drawn to be endpoints. We need to prioritize

our vertices to know which one is under consideration at each step of our bijection. The vertex v under consideration must have the following properties:

- (1) $lv(v) \geq lv(w)$ for all w that have already been included,
- (2) v must not have been declared to be an endpoint,
- (3) v is the vertex farthest to the left such that conditions (1) and (2) hold.

Now that we have f_1 , our three conditions declare that the left child of f_1 is the vertex under consideration. If the second step of D is also a north step, we draw a new family, f_2 coming off of the left child of f_1 . If the second step of D is an east step, we declare that the left child of f_1 is an endpoint and therefore is no longer a viable candidate for parenting a family. We continue this process up our Dyck path until we reach (n, n) . Figure 3.11 shows our example length 14 Dyck path from earlier and the plane binary tree to which f maps it.

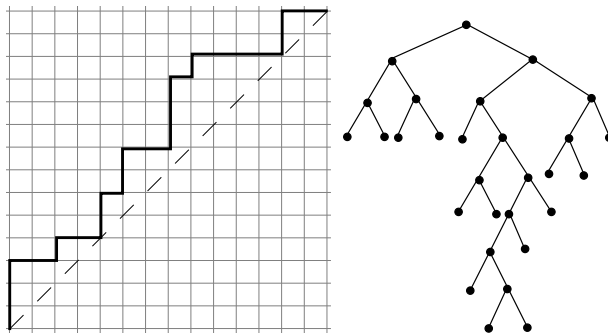


Figure 3.11: A Dyck Path and Its Image Under f

To go from a plane binary tree to a Dyck path, we define $f^{-1} : T_n \rightarrow D_n$ by doing a depth first search, moving from left to right, of the trees. Figure 3.12 shows the order for such a depth first search. We construct our Dyck path by drawing successive north and east steps determined by the vertices of our tree. As we proceed with the depth first search, we add a north step as we come to a parent vertex, and we add an east step as we come to an endpoint. There will be one extra endpoint (since there are $n + 1$ end points and only n east steps), but the Dyck path will be completed before we come to this last endpoint.

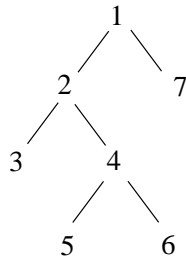


Figure 3.12: A Depth First Search

This bijection, and the others that will be presented in the remainder of the paper, are taken from Stanley[6] and therefore the proof that these are indeed bijections has been omitted. However, it needs to be shown that tarea of the trees corresponds to area of Dyck paths under the bijection; that is, that f is a weight preserving bijection.

Theorem 7. *Let D be a Dyck path of length n . Then $area(D) = tarea(f(D))$.*

Proof. It has already been noted that the n north steps of D correspond to the n families of $f(D)$, and likewise, that the n east steps correspond to the first n endpoints. Let $\vec{g}_D = (a_n, a_{n-1}, \dots, a_1)$ be the g -vector for D . We will construct $\vec{g}_T = (t_n, t_{n-2}, \dots, t_1)$ for the tree $T = f(D)$ such that $\vec{g}_D = \vec{g}_T$. Let t_i be the tarea of the i th family, f_i , of the depth first search of T . From our definition of f^{-1} , we know that f_i corresponds to the i th north step of D . If we can show that $t_i = a_i$, then we are done. In order to do this, we will think of tarea in a less visual way than was presented originally. Claim that $t_i = i - (e_i - 1)$, where e_i is the number of endpoints before f_i in the depth first search. Proving by induction, our base case $t_0 = 1 - (0 - 1) = 0$ is true since we defined $t_0 = 0$. Suppose $t_{i-1} = (i-1) - (e_{i-1} - 1)$. If f_i comes off of the left child of f_{i-1} , then $e_i = e_{i-1}$ and $t_i = (i-1+1) - (e_{i-1} - 1) = i - (e_i - 1) = t_{i-1} + 1$ as desired. If f_i comes off of the right child of f_{i-1} , then $e_i = e_{i-1} + 1$ and $t_i = (i-1+1) - (e_{i-1} + 1 - 1) = i - (e_i - 1) = t_{i-1}$ as desired. We can also say that $a_i = i - (\hat{e}_i - 1)$ where \hat{e}_i is the number of east steps prior to the i th north step as we ascend D . The maximum area that the i th north step can contribute is $i - 1$ and any east step will take away from that area. Since east steps and endpoints directly correspond, and we know from our definition of f^{-1} that the sequence of north steps and east steps for D is identical the sequence of parent vertices and endpoints for T , then $e_i = \hat{e}_i$, and therefore $t_i = a_i$ for all $1 \leq i \leq n$. \square

Since $f : D_n \rightarrow T_n$ is a bijection, $C_n =$ the number of plane binary trees on $2n + 1$ vertices. By the work we have done so far,

$$C_n(q, 1) = \sum_{T \in T_n} q^{\text{tarea}(T)} \cdot 1.$$

Since we found a g -vector, g_T , for plane binary trees, then just as with Dyck paths, g_T holds within its statistics corresponding to dinv and boun . Thus,

$$C_n(q, t) = \sum_{T \in T_n} q^{\text{tarea}(T)} t^{\text{dinv}(T)} = \sum_{T \in T_n} q^{\text{tarea}(T)} t^{\text{boun}(T)},$$

which leads to a new perspective on developing a combinatorial argument for the symmetry of the q, t -Catalan numbers. A similar result follows from the next two objects we discuss.

3.3 Triangulations of Convex $(n + 2)$ -gons into n Triangles

Another object which the Catalan numbers count are *triangulations of convex polygons*:

Definition 39. *Given a convex $(n + 2)$ -gon P , a triangulation of P is a division of P into n triangles using nonintersecting line segments between nonadjacent vertices of P .*

A stipulation that must be made in order for the Catalan numbers to count these triangulations, is that one side of P is designated as the root, or base, side. Therefore, the Catalan numbers count rotations of a triangulated $(n + 2)$ -gon as different objects. Figure 3.13 shows the five distinct triangulations of a $(3 + 2)$ -gon. In this case the bottom horizontal side will denote the root side. Later we will denote the root side by drawing a short, perpendicular line segment through it, as in Figure 3.14.

To show that the Catalan numbers count triangulations of convex $(n + 2)$ -gons we define a bijection $h : P_n \rightarrow T_n$ from triangulations of convex $(n + 2)$ -gons to plane binary trees on $2n + 1$ vertices. For convenience, we rotate the polygon so that the

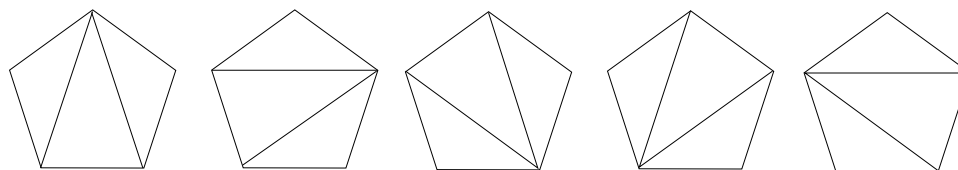
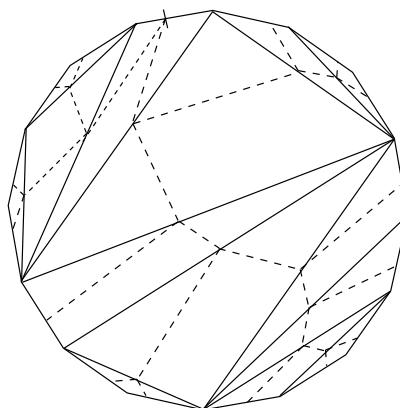


Figure 3.13: The 5 Triangulations of a Pentagon

rooted side is the top most side. Given a triangulated convex $(n + 2)$ -gon, P , we obtain $h(P) = T$ by letting the sides of P along with the interior line segments be the vertices of T . This gives us $(n + 2) + (n - 1) = 2n + 1$ vertices. In fact, the $n + 2$ sides of P correspond with the $n + 1$ endpoints and the vertex of degree 2 of T . Thus, the $n - 1$ interior line segments correspond to the $n - 1$ vertices of degree 3. We let the rooted side of P map to the single vertex of degree 2 of T . At this point, we can draw a vertex on each side and line segment of P . We then draw edges between the vertex of degree 2 and the two vertices which correspond to the two sides of the triangle containing the rooted side. Now we draw in edges from these two vertices to the other sides of the triangles which contain them. Continuing this process until we have covered all the triangles of P results in a unique plane binary tree.

It is a cumbersome task to describe with words $h^{-1} : T_n \rightarrow P_n$, but Figure 3.14 should provide enough illustration to confirm the bijection. This is our same running example. The tree is given by the dashed lines.

Figure 3.14: One Element Under the Bijection $h : P_{14} \rightarrow T_{14}$

3.3.1 Weighted Bijection

Since we know the bijection from plane binary trees to triangulated polygons, we could define a statistic *parea* on polygons which corresponds to *tarea*, and thus area, in very much the same way we defined *tarea* for trees. That is, letting the triangle which contains the rooted side have *parea* 0, and then proceeding to determine the *pareas* of the remaining triangles by the *parea* and side of the triangle from which they came. We can get the same *parea* if we decompose this process into two major steps: Step 1 Standing on the rooted side looking into the interior of the triangulated polygon, darken the line segment coming from the right end of the rooted side. Leave the left line segment alone. Go to either side of this triangle and do the same thing (make certain to come back and do this for the other side as well). Continue until every triangle in the triangulation has been accounted for. Step 2 For each triangle, the *parea* is the number of darkened lines that must be crossed to get from the triangle to the rooted side. *Parea* for the polygon is naturally the sum of the *pareas* for all of the triangles. This is shown in Figure 3.15.

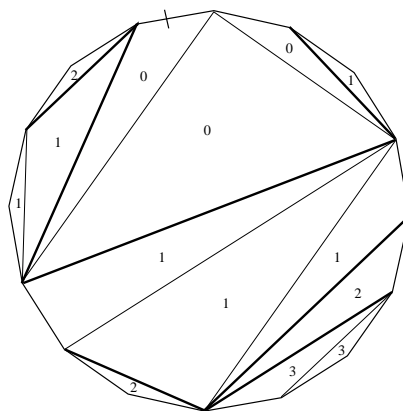


Figure 3.15: The Parea of a 16-gon

Since this corresponds directly to superimposing the tree on the polygon, as in Figure 3.14, and then giving each triangle the *parea* equal to the *tarea* for the family to which it corresponds, $parea(P) = tarea(h(p))$ for all triangulated polygons. The *g*-vector is also preserved under this map.

3.4 Plattices of Length $(n + 1)$

The final combinatorial objects we will investigate are not an extension of the plane binary trees and are more reminiscent of Dyck paths.

Definition 40. A plattice of length $n + 1$ is a set of paired lattice paths in the plane such that

- (a) each path consists of $n + 1$ unit steps,
- (b) each unit step is either a north step or an east step, and
- (c) the paths intersect at exactly their end points.

Let L_n denote the set of all plattices of length $n + 1$.

It may be helpful to refer to each path as either the *upper* or the *lower* path. Figure 3.16 shows four examples of paired lattice paths. Sets 1 and 4 are plattices of length 8. 2 is not, since the two paths intersect in a point other than their end points. 3 is not, since the upper path contains a south step (it also contains more unit steps than the lower path). Notice that the upper path of 2 is the same as the upper path of 1, and that the lower path of 2 is the lower path of 4. Both 1 and 4 are plattices, so creating plattices is more than just pairing together paths with suitable lengths.

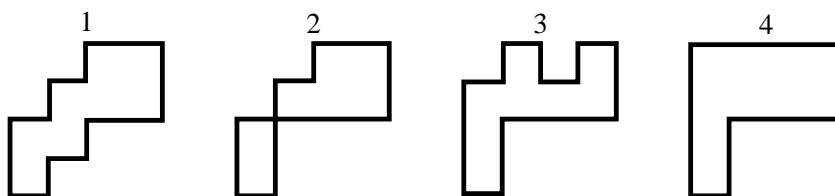


Figure 3.16: Four Sets of Paired Lattice Paths

Instead of thinking of plattices as two conjoined paths, we can think of them as the polygons formed by these paths. We can divide these polygons into unit squares in order to define a statistic, *plarea*, on plattices.

Definition 41. The *plarea* of a unit square of a plattice is the number of unit squares vertically between it and the lower path. The *plarea* of a plattice, L , is given by

$$\text{plarea}(L) = \sum_{u_i} \text{plarea}(u_i),$$

where the sum is taken over all unit squares, u_i , which have at least one side in common with the upper path of L .

The plareas of plattices 1 and 4 from before are shown in Figure 3.17. Plattice 1 has a plarea of 4 while plattice 4 has a plarea of 9.

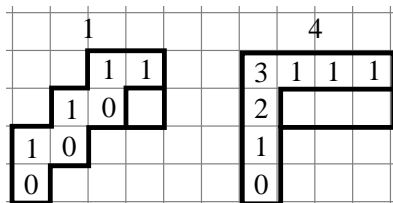


Figure 3.17: Plarea for Two Plattices of Length 8

3.4.1 Weighted Bijection

We define a bijection $j : D_n \rightarrow L_n$ from length n Dyck paths to plattices of length $n + 1$. Given a Dyck path, D , we first locate all outside corners of D . Then for each outside corner, we place an X in the unit box in the corner and every unit box below it, down to and including the box on the line $y = x$. This is shown in Figure 3.18 for our example Dyck path of length 14. This process gives us two sets of vertical columns: those that have been filled in with X 's and those that have not.

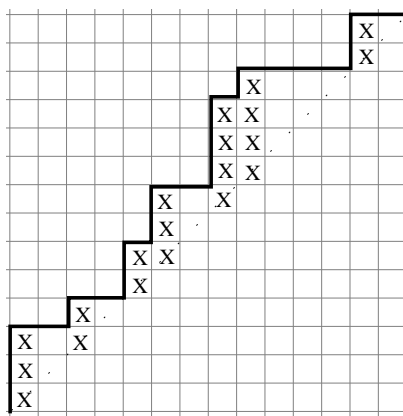


Figure 3.18: The First Step of $j : D_n \rightarrow L_n$

We then remove from D each vertical column of X 's one at a time from left to right. It does not really matter where we put the first column as long as it remains vertical. Before removing the second column of X 's, we count the empty columns between it and the first column. Supposing there are m empty columns between them, we place this second column immediately to the right of the first column but up m units from the bottom of the first column. We continue this process up our Dyck path, letting the number of empty columns determine the vertical shift between successive columns. Formally, the outline of this new shape is our plattice, $j(D)$. Figure 3.19 shows this for our example Dyck path, but the X 's which correspond to the area of a given row have been replaced with the row areas. These areas are mapped directly to the plareas of each unit square of the plattice. Thus, the g -vector is preserved as it snakes it way from the bottom to the top of the plattice.

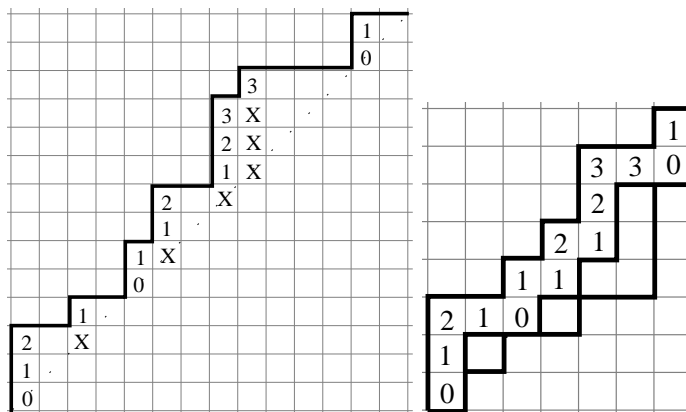


Figure 3.19: $\text{area}(D) = \text{plarea}(j(D))$

Since we have preservation of the g -vector, we can determine statistics which correspond to dinv and boun . The statistic plinv which corresponds to dinv , would be

$$\text{plinv} = \sum_{i=0}^n \binom{|i|}{2} + |i + 1 \triangleright i|,$$

where $|i + 1 \triangleright i| =$ the number of i 's to the right of $i + 1$ in the plattice. We could make a similar argument for a bounce statistic.

Bibliography

- [1] Fulton, William. *Young Tableaux*. Cambridge University Press, Cambridge, 1997.
- [2] Haglund, James. *The q, t -Catalan Numbers and the Space of Diagonal Harmonics*. American Mathematical Society, Providence, 2008.
- [3] Haglund, James. *Conjectured statistics for the q, t -Catalan numbers*. *Advanced Mathematics* 175(2003), 319-334.
- [4] MacMahon, P. A. *Combinatory Analysis*. Cambridge University Press, London, 1918.
- [5] Sagan, Bruce E. *The Symmetric Group: Representations, Combinatorial Algorithms, and Symmetric Functions*, Second Edition. Springer Science + Business Media, LLC, New York, 2001.
- [6] Stanley, Richard P. *Enumerative Combinatorics*, Volume 2. Cambridge University Press, Cambridge, 1999.
- [7] Stembridge, John. *The SF Package*, version 2.4. Available at <http://www.math.las.umich.edu/~jrs/maple.html>.

Vita

Kristy L. Beam

Personal Information

Born: December 8, 1985, Hickory, North Carolina
Undergraduate Study: Lenoir-Rhyne College
Hickory, North Carolina
B.S. *Magna Cum Laude*, Mathematics, May 2007
Graduate Study: Wake Forest University
Winston-Salem, North Carolina
M.A., Mathematics, May 2009

Presentation

“Pascal’s Carousel” presented March, 2007, MAA Southeast Regional Meeting, Statesboro, GA.

Honors and Awards

Pi Mu Epsilon Inductee, Wake Forest University, 2008
Honors Thesis Award, Lenoir-Rhyne College, May, 2007
Fritz Mathematics Award, Lenoir-Rhyne College, May, 2007
Patterson Prize for Outstanding Undergraduate Paper Presentation, MAA Southeast Regional Meeting, March, 2007

Academic Organizations

American Mathematical Society
Association for Women in Mathematics